Seventh FRAMEWORK PROGRAMME THEME 6 Environment

Collaborative Project (Large-scale Integrating Project)

Project no. 212085

Project acronym: **MEECE**

Project title: Marine Ecosystem Evolution in a Changing Environment

D3.4 Synthesis report for Climate Simulations

Part 6: Bay of Biscay

Due date of deliverable: 30/08/2012

Actual submission date: 08/02/2013

Lead partner responsible for deliverable: AZTI-Tecnalia

Project co-funded by the European Commission within the Seventh Framework Programme, Theme 6 Environment		
Dissemination Level		
PU	Public	x
PP	Restricted to other programme participants (including the Commission)	
RE	Restricted to a group specified by the consortium (including the Commission)	
CO	Confidential, only for members of the consortium (including the Commission)	

Start date of project: 01.09.09 Duration: 54 months (including extension)

Project Coordinator: Icarus Allen, Plymouth Marine Laboratory

D3.4 Synthesis report for Climate Simulations

Part 6: Bay of Biscay

Contributors:
Marina Chifflet[1], Igaratza Fraile[1], Guillem Chust[1], Luis Ferrer[1], Yolanda Sagarminaga[1], and Philippe Verley[2]
[1] AZTI-Tecnalia, Spain
[2] IRD, France

Collaborators:
Xabier Irigoien (KAUST, Saudi Arabia)

Table of contents

1. Science questions

The productivity of the Bay of Biscay pelagic ecosystem is strongly dependent on hydro-climate processes and freshwater inputs. However, our predictive ability in these areas remains weak. How natural climate variability or anthropogenic climate change may affect the dynamics of the pelagic ecosystem need to be evaluated in order to provide sound advice to managers. This is a crucial step in order to anticipate how climate change may alter the global productivity of the Bay of Biscay.

Hydro-climate processes, such as haline-stratification and nutrient inputs both due to river discharges, mesoscale activity over the slope and mixing or stratification, are thought to be largely responsible for the high variability in planktonic production and dynamics. Moreover, environmental conditions and low-trophic-level structure and production, and hence their variability, have an important role on the high-trophic-level productivity and population distribution and structure. In the Bay of Biscay, the pelagic fish key-species form the basis of important fisheries that represent an important source of income for local economies. These species are mainly: anchovy, sardine, mackerel, horse mackerel, blue whiting and hake. Thus, it is crucial to understand the natural variations in these fish stocks abundance and productivity. One of the main objectives is to assess the response of high-trophic-level productivity and ecosystem structure to the variations of low-trophic-level and hydro-climate processes. This has been considered in a multispecies context, using an end-to-end model, where conditions that are detrimental for one species can be favourable for another.

2. Model description

2.1. Lower Trophic Level: ROMS+$N_2P_2Z_2D_2$

For the simulations described and delivered in the frame of WP3 and WP4 of MEECE, the high resolution 3D prognostic ocean model ROMS (Regional Ocean Model System, Shchepetkin & McWilliams, 2005), forced by detailed atmospheric, hydrologic and oceanic forcing, has been used. The model domain covers the entire Bay of Biscay, extending from the French and Spanish coasts (40.5 ^{o}N) to the South of United Kingdom (52.5 ^{o}N) and to 13 ^{o}W (Fig. 1). In the present configuration for the Bay of Biscay, an extension of a configuration is limited to the South Bay of Biscay (Ferrer *et al*., 2009). The bathymetry has been obtained by interpolation of the ETOPO2 (2 minute digital Elevation TOPOgraphic model, Smith & Sandwell, 1997), GEBCO (General Bathymetric Chart of the Oceans), and IBCM (International Bathymetric Chart of the Mediterranean) data sets. ROMS for Bay of Biscay computes the primitive equations on a 6.6-km grid in the horizontal and 32 no-equally distributed σ–levels grid in the vertical.

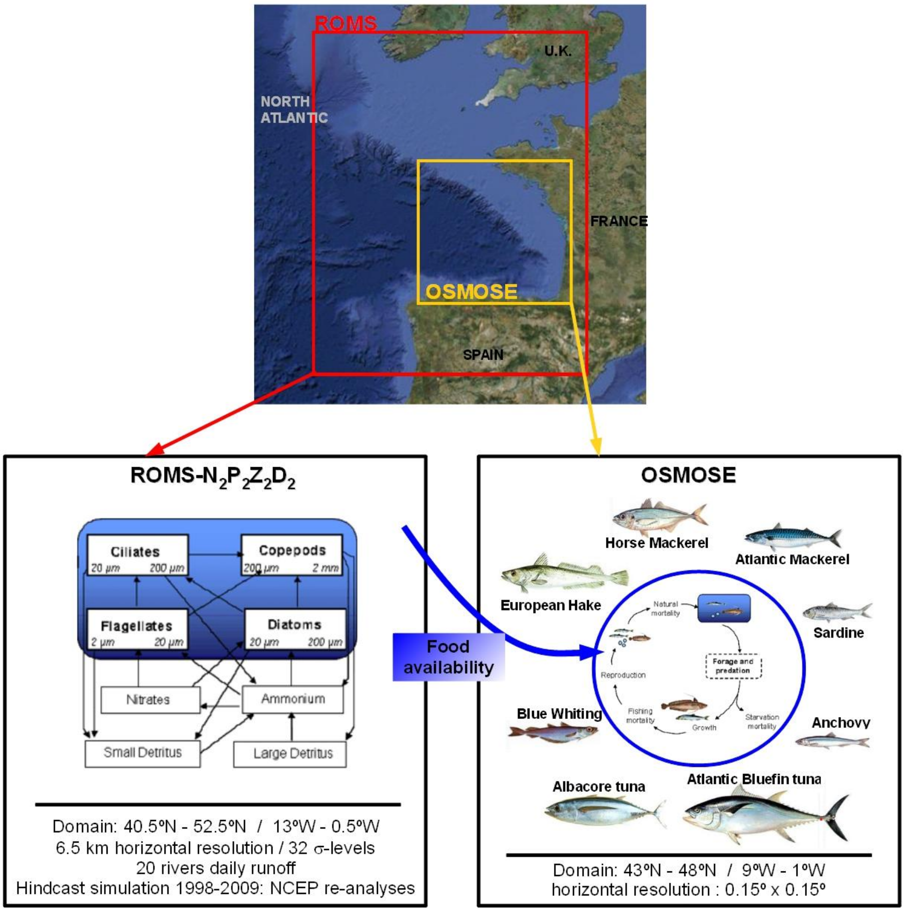

Figure 1: Synthesis scheme of the end-to-end model implemented in the Bay of Biscay: ROMS-$N_2P_2Z_2D_2$ and OSMOSE domains and specificities. 6 biogeochemical variables are included in the NPZD model, and 8 species in the OSMOSE model. The ROMS-$N_2P_2Z_2D_2$ provide the prey fields to the OSMOSE model.

The river runoff data are prescribed as boundary conditions on momentum, salinity, temperature and nitrate. Daily flow data are used from observations in the 20 most important rivers on the French and Spanish coasts. The temperature and nitrate concentrations of these rivers are prescribed from observations when available and using monthly means.

ROMS is coupled to a $N_2P_2Z_2D_2$ biogeochemical model, taking into account ammonium, nitrate, 2 classes of phytoplankton, 2 classes of zooplankton and 2 classes of detritus.

2.2. Higher Trophic Level: OSMOSE

The higher trophic level model applied to the Bay of Biscay is the OSMOSE (Object-oriented Simulator of Marine ecOSystems Exploitation) model. Details of the system are provided in the MEECE deliverable D2.3 (*"Sub-model OSMOSE, Functional coupling with plankton models"*). OSMOSE is a 2D, multispecies and Individual-Based Model (IBM) which focuses on fish species. It models processes of growth, predation, reproduction, natural and starvation mortalities, and uses the outputs of the LTL model ROMS-$N_2P_2Z_2D_2$ as prey fields (Fig. 1). A total of 8 fish species are included, from small pelagic to top predators: *Engraulis encrasicolus, Sardina pilchardus, Trachurus trachurus, Scomber scomber, Merluccius merluccius, Micromesistius poutassou, Thunnus thynnus*, and *Thunnus alalunga* (Fig. 1). OSMOSE has been implemented in the Bay of Biscay, between 43-48^o N and 1-9^o W, with a spatial resolution of 0.15^o x 0.15^o. Temporal resolution is 15 days. Detailed information of species distribution in terms of presence/absence data by age and time step has been extracted from literature. The implementation and calibration of the OSMOSE model in the Bay of Biscay have been undertaken by AZTI with the collaboration of Yunne Shin and Philippe Verley (IRD, France). A genetic algorithm has been used to calibrate OSMOSE (collaboration with Philippe Verley, IRD, France) to allow calculation of larval additional mortalities and plankton accessibilities.

3. Scenarios: model validation and projections

We consider three model experiments: a hindcast simulation forced by the re-analysis NCEP atmospheric forcing and two IPSL-CM4 forced climate simulations (CNTRL and A1B).

3.1. Hindcast simulation

Lower Trophic Level

A 13-year simulation has been performed, from 1997 to 2009, using the 6-hours NCEP re-analysis as atmospheric forcing (Kalnay *et al.* 1996): air temperature, winds, pressure and humidity, and short-wave radiation. The initial boundaries conditions for currents, temperature and salinity are interpolated on the grid from the World Ocean Atlas 2005 (WOA05) developed by the National Oceanographic Data Center (NODC) of the NOAA. The water level is specified for initial condition and also at each time step along the open boundaries, using the OSU TOPEX/Poseidon Global Inverse Solution version 5.0 (TPXO.5, global model of ocean tides). After a 1-year spin-up (year 1997) to reach equilibrium, the simulation covers the period 1998-2009, with 1 year of spin-up and a time step of 15 minutes.

The runoff data of the 20 most important rivers in the Bay of Biscay are prescribed as boundary conditions on momentum, salinity, temperature and nitrate. The daily flow observations have been extracted from databases: HYDRO II (France), and databases of “Diputación Foral de Gipuzkoa” and “Diputación Foral de Vizcaya” (Spain). Moreover, monthly climatologies of temperature and nitrate have been calculated using the *in situ* observations from the same databases, and prescribed in the simulation as boundary conditions at river points.

Higher Trophic Level

A hindcast reference simulation has been undertaken using the prey fields from the 1998-2009 hindcast ROMS-$N_2P_2Z_2D_2$ simulation: small and large phytoplankton and zooplankton. A climatologic year has been repeated during 50 years to reach equilibrium (Fig. 2). Since the OSMOSE model presents stochastic parameterization, 10 replicates of the 50 years reference simulation are computed at the same time. Thus, each resulted variable (e.g. fish biomass and abundance, and fish diet) is the mean of the 10 replicates. The equilibrium is reached after 25 years of spin-up (Fig. 2). That is to say that after 25 years of spin-up, the time evolution for each species is stable and only present the seasonal cycle. Since the 50 years simulation with OSMOSE does not represent a time evolution but the repetition of the same climatologic year (50 times), this climatologic year is calculated using the last 25 years of the simulation (from 26th to 50th years).

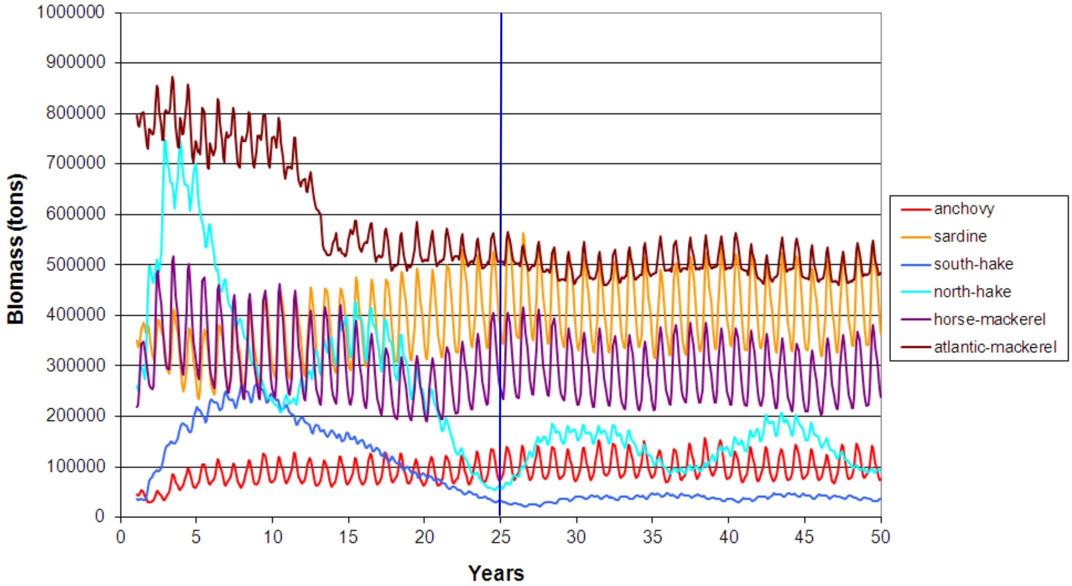

Figure 2: Evolution of fish biomasses over 50 years simulation – spin-up of 25 years.

3.2. Climate change simulations

LTL model ROMS-$N_2P_2Z_2D_2$

The climate change experiments (CNTRL and A1B) were performed using results from the IPSL-CM4 model (D1.2). The control simulation (CNTRL) is a 21-year present-day run for the period 1980-2000, using atmospheric IPSL-CM4 model outputs for the LU20C2 simulation. Tides and rivers match those in the hindcast simulation. The future climate simulation (A1B) is a 20-year run for the period 2080-2099, using atmospheric IPSL-CM4 model outputs for the LUA1B1 simulation. This future climate simulation represents possible conditions in 2080-2099 under a Business as Usual emissions scenario. Last year of daily runoff observations (year 2009) is repeated beyond the period.

HTL model OSMOSE

The climate simulations are performed with OSMOSE using the prey fields from the 1980-2000 and 2080-2099 ROMS-$N_2P_2Z_2D_2$ climate simulation. As for the hindcast simulation, small and large phytoplankton and zooplankton have been used, and a climatologic year is calculated using the last 25 years of each simulation (from 26th to 50th years).

Downscaling method

Direct usage of the IPSL-CMA4 outputs has been selected as downscaling to force the LTL model (D3.1, 3.1.3 A. Direct forcing).

4. Metrics considered and validation

Considered variables:

- Temperature (SST (^{o}C)) (absolute difference) and seasonal stratification (strength and period length)
- Circulation: seasonal patterns of the surface and sub-surface circulation
- Nutrients (fractional change): nitrate and ammonium
- Phytoplankton (small and large, Biomass Depth integrated (mg/m^2) (fractional change)
- Zooplankton (small and large, Biomass Depth integrated, mg/m^2) (fractional change)

Validation techniques

To validate the model, we adopted methods proposed by the MEECE deliverable D2.7.

In order to validate the LTL model results, we have compiled *in situ* data and remotely-sensed information:

- AVHRR SST – 1982-2008 period
- Sea surface chlorophyll a concentration from satellite SeaWIFS – 1997-2009 period
- Sea surface chlorophyll a concentration from satellite MODIS – 2002-2009 period

Thus, simulated results have been sampled for the same dates and geographical positions and interpolated to observation positions and depth levels, for each year of the hindcast simulation, from 1998 to 2009. To assess model skill and to obtain a synthetic view of comparison/validation, we applied Taylor diagrams (Taylor, 2001) to visualize model performance (hindcast simulation) with respect to observations.

CPR zooplankton data have not been used since samples are very scarce within the Bay of Biscay.

5. Linkages with MEECE deliverables

The MEECE deliverables listed in Table 1 were used to undertake the present deliverable part.

Table 1. Linkages with MEECE deliverables.

Deliverable	Comments
D1.2	IPSL-CM4 model outputs and manual
D1.4	Fishing scenarios: OSMOSE parameterization for Fmsy and Fpa
D1.6	Hindcast + present day climate + future climate (A1B1 - IPSL-CM4)
D1.3	- Satellite images - *In situ* AZTI's cruises observations (not from the D3.1)
D2.3	OSMOSE model
D3.1	Common set of forcing scenarios
D3.2	Common set of metrics

6. Results

6.1. Hindcast simulation and validation

Climate and physical variables

In terms of hydrology, the 12-years monthly mean simulated SST has been compared to monthly climatology from AVHRR, using Taylor diagram and P*bias* (Fig. 3). The Taylor diagram between simulated monthly mean SST and AVHRR monthly climatology shows a correlation between 0.8 (July-August) and 0.9, and a normalized standard deviation between 0.75 and 1.25. Therefore, the model reproduces the overall seasonal cycle of SST in the Bay of Biscay. At spatial basis, the model fits also well the local processes: cold band water along the Atlantic French coast in winter, warming and north-south gradient in spring, Galician upwelling, Ouessant front and cold slope band in summer, and rivers plumes.

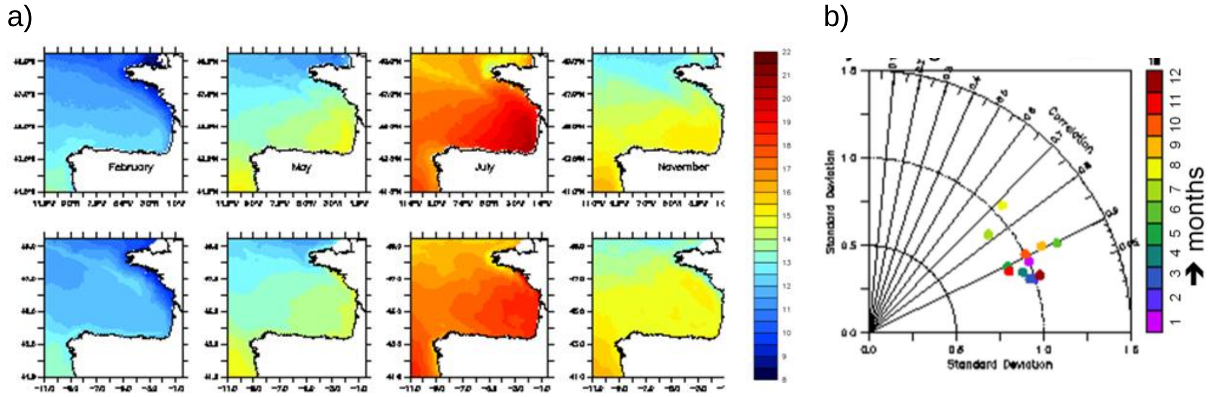

Figure 3: Sea Surface temperature: assessment of the model simulation quality against the 1998-2008 AVHRR observations: a) maps of SST from AVHRR (upper panels) and ROMS (lower panels) for February, May, July and November; b) Taylor diagram per month.

The model reproduces the main circulation patterns in the Bay of Biscay, and meso-scale processes (Fig. 4): a strong poleward slope current in autumn-winter, a slow circulation over the shelf, eddies formation from the slope towards the plain, the Galician upwelling west of Spanish coast in summer, and a strong jet coastal current along the coast in autumn (September to October) observed by Lazure et al. (2008). Moreover, the comparison of simulated surface circulation to RADAR observations during spring 2008 and 2009 shows a strong interannual variability of the slope current. The model reproduces the main shift in the circulation.

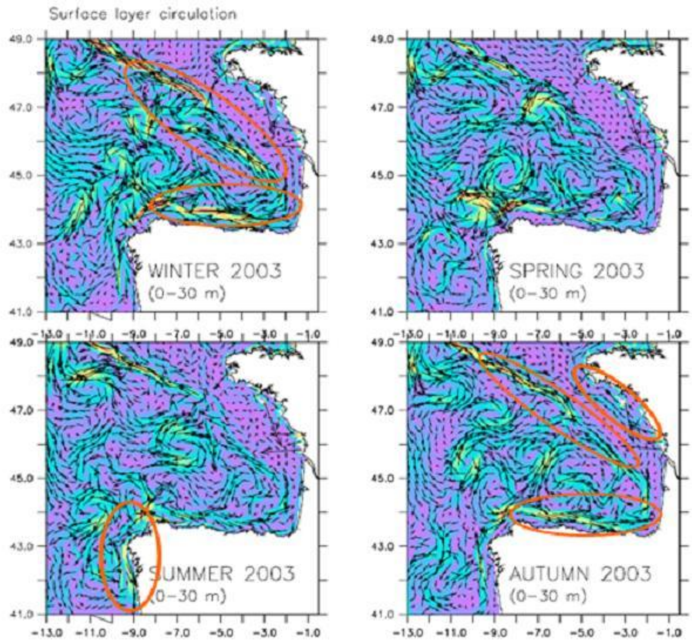

Figure 4: Simulated surface global circulation in the Bay of Biscay for the four seasons. The main circulation patterns are enclosed in red lines.

Lower Trophic Level

The hindcast validation of the lower trophic level (LTL) encompasses times series of nutrients, phyto- and zooplankton concentrations. The domain-averaged time series of integrated nitrate concentration, primary production, phytoplankton and zooplankton biomass present an important interannual variability (Fig. 5a,b,c). The model produces a mean seasonal cycle of phytoplankton biomass and nitrate concentration coherent with the observations in the region. A strong interannual variability in the timing and the duration of the bloom, and especially in the maximum value of chl-*a* biomass (*e.g.* phytoplankton biomass) is simulated: strong and early blooms in 1998, 2005, 2006 and 2009, associated to high values of integrated nitrate concentrations; some years as 2000 and 2008 present two peaks of chl-*a*. The comparison of the simulated surface chl*a* to SeaWiFS and MODIS observations, from 2001 to 2009, indicates a well captured interannual variability by the model, although a too early (about 1 month) simulated spring bloom (Fig. 5d). As an example, the strong spring blooms in 2005 and 2009 were reproduced by the model and also the earlier onset in 2005. Moreover, no validation has been undertaken for the nitrate concentration because of lack of available data in the region.

a) Nitrate 0-200 m concentration (mmol.N m^{-2})

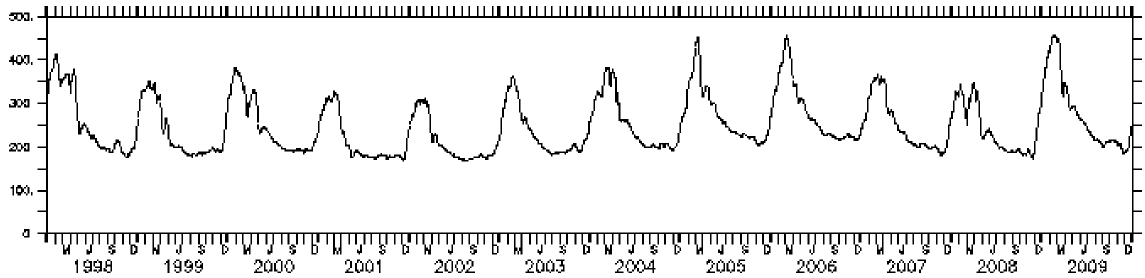

b) Large (black) and small (blue) 0-200 m phytoplankton concentration (mmol.N m^{-2})

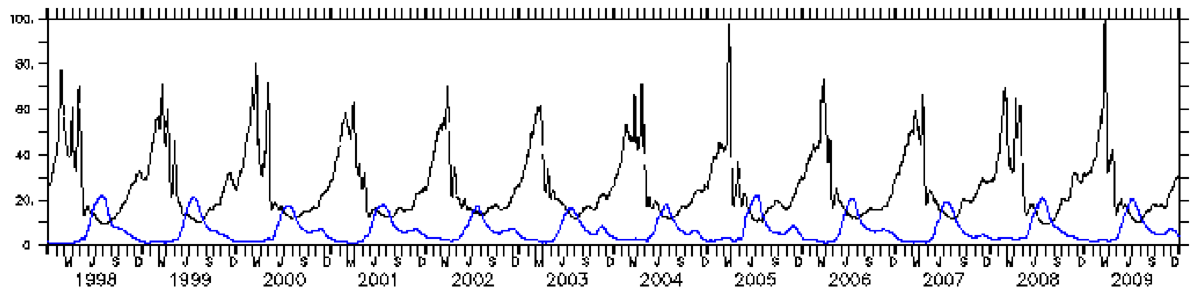

c) Large (black) and small (blue) 0-200 m zooplankton concentration (mmol.N m^{-2})

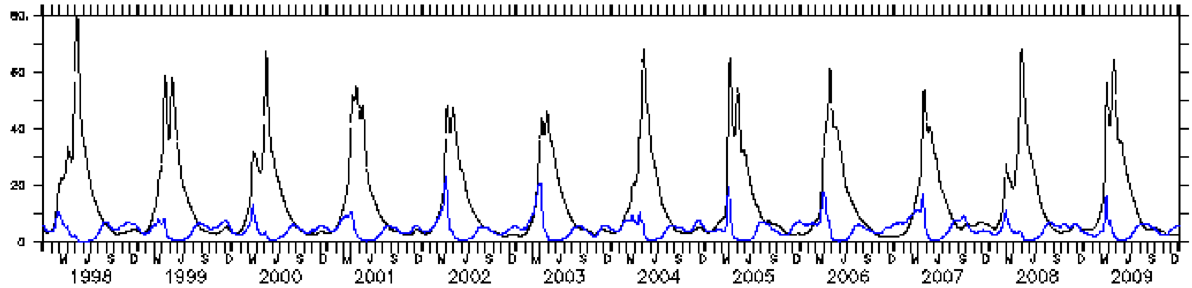

d) Comparison of monthly mean surface chlorophyll-*a*, horizontally domain-averaged: simulated by ROMS (black line), and observed with SeaWiFS (blue line) and MODIS (red line) sensors.

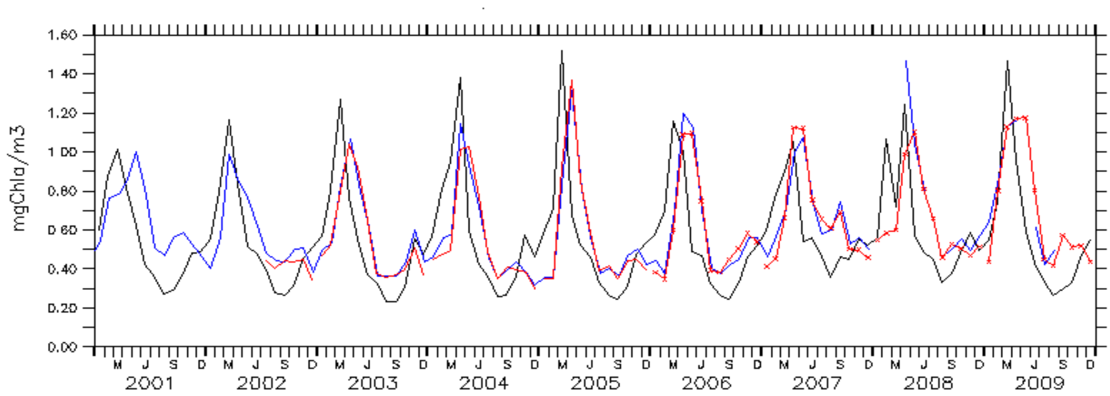

Figure 5: Times-series and horizontally domain-averaged (0.5-10.5 ^{0}W / 42-49 ^{0}N) of: a) simulated integrated nitrate concentration; b) simulated integrated phytoplankton concentration; c) simulated integrated zooplankton concentration; d) Comparison of monthly mean surface chlorophyll-a, horizontally domain-averaged: simulated by ROMS (black line), and observed with SeaWiFS (blue line) and MODIS (red line) sensors.

Higher Trophic Level

The seasonal evolution of the biomass shows higher values in spring-summer than in winter (Fig. 6). Simulated sardine and Atlantic mackerel represent the higher stocks in the Bay of Biscay. The mean anchovy biomass varies between 70000-8000 in autumn-winter and 140000-150000 tons at its maximum in May-June. Thus, the seasonal oscillation of anchovy biomass is *ca*. 70000 tons (50%). The mean sardine biomass varies between 300000-350000 in January-February and 500000-520000 tons at its maximum in June-July. The seasonal oscillation of sardine biomass represents about 40% (200000 tons) of its total biomass.

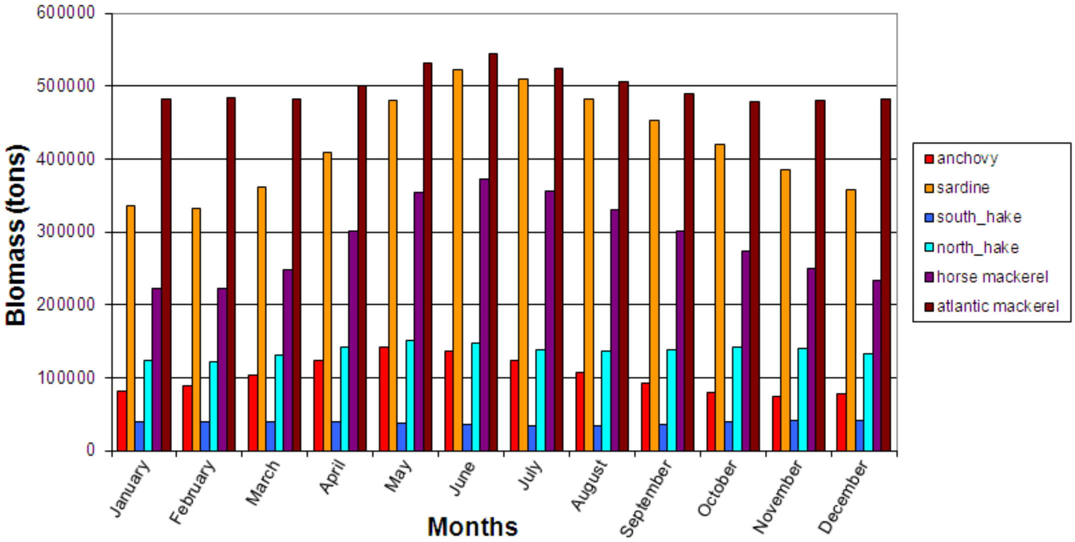

Figure 6: Seasonal evolution of fish biomass simulated by OSMOSE. Results over a climatologic year corresponding to the hindcast 1998-2009.

6.2. Climate forced simulations

Atmospheric environment

Table 2 shows the comparison for the wind velocity (ms^{-1}) and the air temperature (ºC) between *i)* the NCEP-reanalyzes and the IPSL-CM4 global model outputs for the same period 1998-2000, and *ii)* the IPSL-CM4 global model outputs for 1980-2000 (present or CNTRL) and 2080-2099 (future or A1B).

For the period 1998-2000, the IPSL local wind is lower than the NCEP-reanalysis (hindcast) of about 1.8 ms^{-1}. The difference between IPSL-CNTRL wind and IPSL-A1B wind is 0.25 ms^{-1}, i.e. lower than the difference between NCEP re-analysis and IPSL-CNTRL values. As for the wind, we observe a large difference between the IPSL-CNTRL air temperature and from the NCEP-reanalysis: there is 2.6 ºC of difference for the three overlap years. The difference between IPSL-CNTRL and IPSL-A1B air temperature is 2.84 ºC, the same order of magnitude than the difference between NCEP-reanalyzes and IPSL-CNTRL.

Thus, the IPSL-CM4 global model results for the Bay of Biscay do not fit with the NCEP reanalyzes. The climate study will thus be done using the both IPSL-CM4 scenarios simulations (CNTRL 1980-2000 and A1B 2080-2099), focusing on the differences between them and not on the absolute values.

Table 2. Comparison of the wind velocity (m s^{-1}) and the air temperature (ºC), from the NCEP-reanalyzes database and the IPSL-CM4 global model, and for the “present” and “future” periods.

	Mean wind speed (m s^{-1})	**Mean air temperature (ºC)**
NCEP 1998-2000	8.06	13.21
IPSL-present 1998-2000	6.27	10.60
IPSL-present 1980-2000	6.12	10.30
IPSL-future 2080-2089	5.87	13.14

Environmental variable SST

The climate change signal between A1B and CNTRL is characterized by a general increase of the SST (Fig. 7). The SST increases with a mean value of about 3.5 ^{o}C for the whole domain (see Table 3 in last section). The spatial variability of the warming is very strong. On the Armorican and Aquitaine shelf (French coast), the warming is the stronger with SST increase above the mean value of 3.5 ^{o}C. Over the slope and along the north and west Spanish coast, the warming is lower with values between 1 and 3.5 ^{o}C. The upwelling region off Galicia (west of Spain) is the area with the lower warming. This simulated spatial variability is in accordance with the POLCOMS-ERSEM model results in the Bay of Biscay (D3.4 Part 3).

(a) (b)

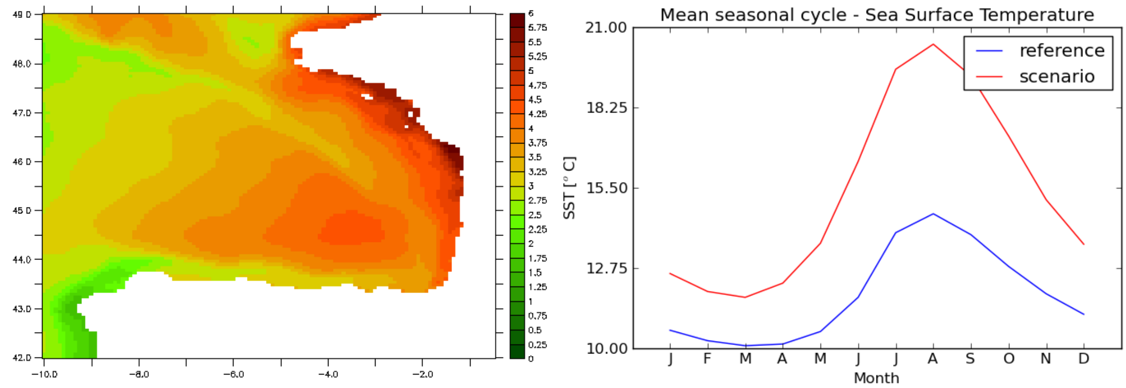

Figure 7: a) Simulated absolute difference between 2080-2099 and 1980-2000 periods for SST (ΔºC); b) Comparison of the annual cycle of SST for the both periods.

Phytoplankton and zooplankton biomass

The changes in phytoplankton biomass are also spatially variable (Fig. 8a). The phytoplankton biomass decreases on the French shelf and south-eastern corner of the bay, and on the central plain, while it increases along the slope (except for a small part in the SE of the bay), and on the West part of the domain. The changes in phytoplankton biomass present mesoscale patchiness and slight increase close to some river mouths (*e.g.* Vilaine, Loire), and patches of decrease in the north-west part of the domain (west of Brittany). The changes in zooplankton biomass present some differences (Fig. 8b). The zooplankton biomass increases in the major part of the domain, except on the French shelf (Armorica and Aquitaine Shelves). It presents also patches of increase close to some river mouths.

Both the annual cycle of phytoplankton and zooplankton biomass are modified (Fig. 8c,d). A large shift in the seasonal cycle is simulated for the phytoplankton and the zooplankton, with a time advance of 2 months for the spring bloom maximum in A1B (scenario) in comparison with CNTRL (reference): the maximal value of phytoplankton biomass happens in March in A1B instead of May in CNTRL, and the maximal value of zooplankton happens in April in A1B instead of June in CNTRL.

However, there is no clear trend in terms of intensity. The phytoplankton biomass maximum slightly decreases while zooplankton increases of *ca*. 14% (maximum of 400 mgC m^{-2} compared to 350).

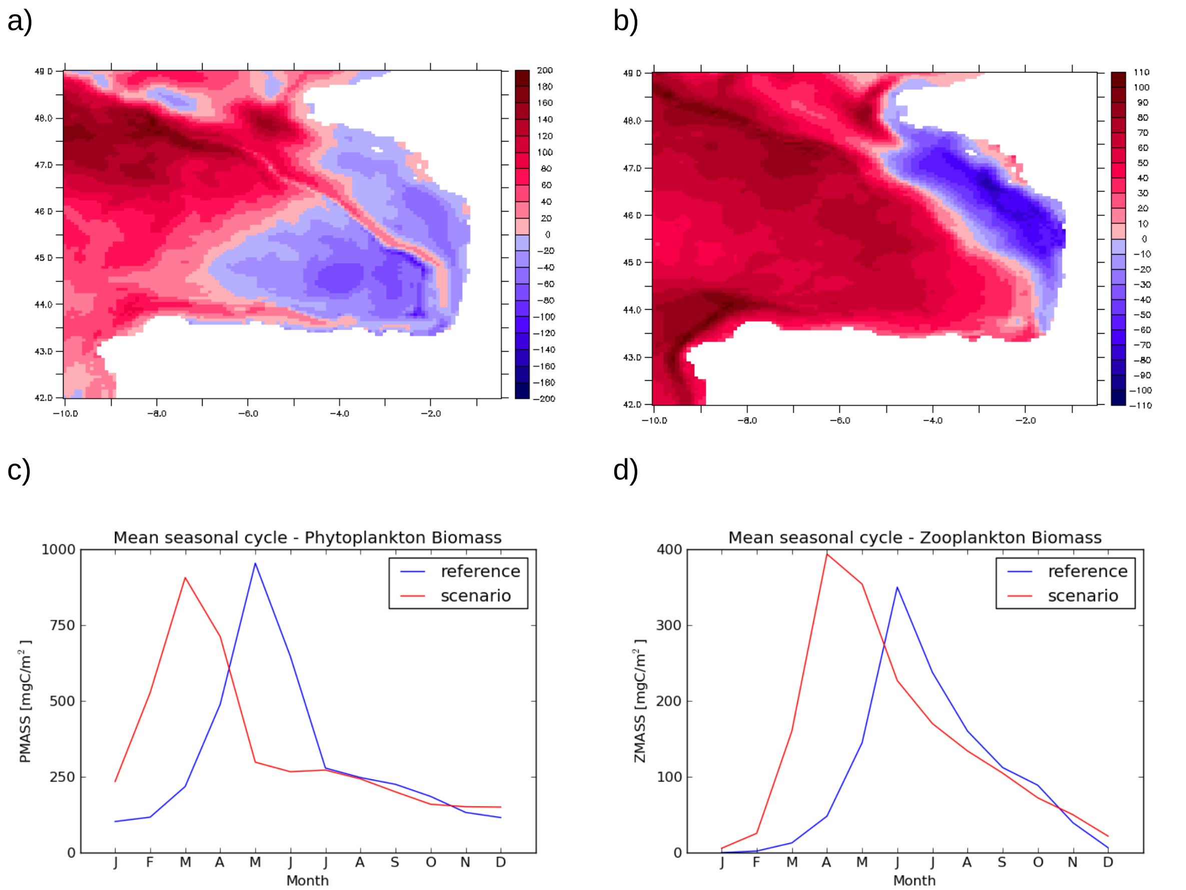

Figure 8: Simulated absolute difference between 2080-2099 and 1980-2000 periods for: (a) 0-500 m phytoplankton biomass (mg C m^{-2}) and (b) 0-500 m zooplankton biomass (mg C m^{-2}); Comparison of the annual cycle between the two periods (Δ mg C m^{-2}) for (c) phytoplankton biomass and (d) zooplankton biomass. "Reference" is the CNTRL run and "scenario" the A1B run.

Fish biomass

Total fish biomass simulated by OSMOSE for the whole Bay of Biscay increases by 4.6% (Fig. 9). While most of species increase (anchovy: 22%, sardine: 15%, and specially hake by 33%), the stock of Atlantic mackerel and horse-mackerel decrease slightly (-5%). This slight increase in total fish biomass, compared with the high increase in overall zooplankton (44%) is explained because of the spatial variability in zooplankton change. Thus, in the French shelf, zooplankton is expected to decrease and peak earlier in the year and also it is the main area of spawning fish species at present day climate (Aldanondo et al., 2010). For instance, European anchovy in the Bay of Biscay spawn primarily in highly productive areas, such as river plumes, especially under the influence of large French rivers (Gironde and Adour), and partially on the shelf (Aldanondo et al. 2010). Moreover, the spawning season of European anchovy extends from March to August with a maximum intensity peak between May and June (Motos, 1996; Bellier et al., 2007). Since the maximal value of zooplankton would occur earlier (i.e. April) in the future scenario than at present day climate (i.e. June), this could also produce a mismatch between anchovy larvae growth and zooplankton bloom. This type of mismatch is critical for the population growth and has been reported, for instance, for Atlantic cod in the North Sea (Richardson, 2008).

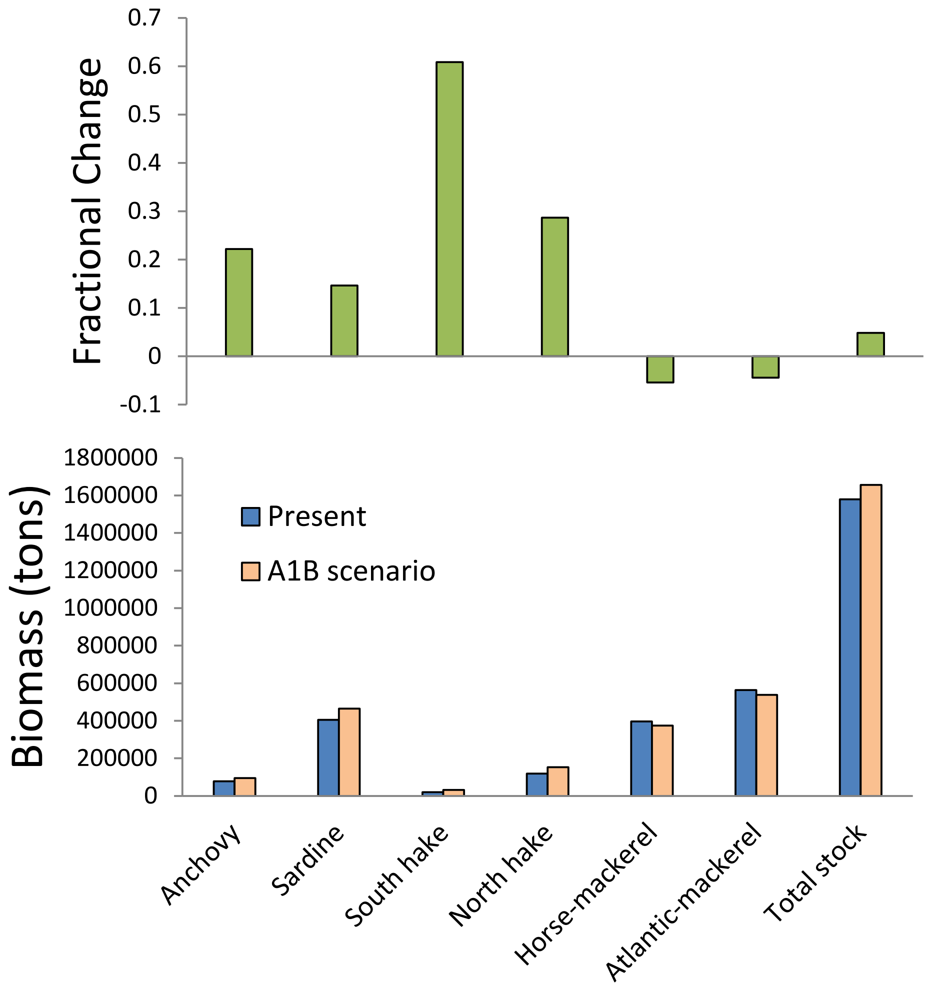

Figure 9: Fish biomass and fractional change from OSMOSE simulations: CNTRL climate (1980-2000) and A1B climate (2080-2099).

7. Discussion

The main physical change for the climate simulation A1B (2080-2099) is an increase of the SST of about 3.5 ^{o}C, with moderate spatial variability. This increase is slightly higher than that expected using POLCOMS-ERSEM (2.2 ^{o}C, see D3.4 Part 3, and Holt et al. 2010) and model ensembles (1.5 to 2.1 ^{o}C, see Chust et al. 2010, 2011).

Phytoplankton and zooplankton biomasses increase globally although with a strong spatial variability: (*i*) on the French shelf, the phytoplankton and zooplankton biomass decrease; (*ii*) offshore, the phytoplankton decreases at the centre of the bay and increases elsewhere (south part, and north and west parts) while the zooplankton increases in all the offshore plain; (*iii*) on the shelf break, both phytoplankton and zooplankton increases.

These results concerning phytoplankton and zooplankton are slightly in disagreement with the POLCOMS-ERSEM model (see D3.4 Part 3, and Holt et al. 2012) results mainly for two important zones:

- Over the slope, the POLCOMS-ERSEM model simulates a decrease of both phytoplankton and zooplankton while the ROMS-NPZD model simulates an increase.
- On the south-western part of the domain (especially off Galicia and along the Spanish shelf), the POLCOMS-ERSEM model simulates a decrease of both phytoplankton and zooplankton while the ROMS-NPZD model simulates an increase.

The difference of resolution of the both models could explain in part the different results, as the slope is very strong in the Bay of Biscay and the Spanish shelf very narrow.

The expected slight increase in total fish biomass, which has important consequences in terms of local fisheries, is a response of overall increase in phytoplankton and zooplankton biomass projected by ROMS-NPZD model. However, POLCOMS-ERSEM model projected no significant change in primary and secondary production (see D3.4 Part 3), which could have slightly different results for overall fish biomass. Thus, climate change projections for the higher trophic level of the Bay of Biscay are still uncertain although it constitutes the first attempt, as far as we know, of evaluating quantitatively future climate change impacts to fish stocks in the area at high spatial and temporal resolution (see a review in Chust et al., 2011).

Previous long-term studies have shown that population dynamics of practically all species of commercial interest within the Bay of Biscay are influenced by climate. For instance, factors such as the North Atlantic Oscillation (albacore, Arregui et al. 2006; sardine, Alheit & Hagen 1997; several fish stocks, Hemery et al. 2008), EA pattern (in anchovy, Borja et al. 2008); temperature anomaly (hake, Fernandes et al. 2010), upwelling strength (anchovy, Borja et al. 2008), turbulence (anchovy, mackerel and hake, Allain et al. 2007, Fernandes et al. 2010, Andonegi et al. 2011), river discharge (anchovy, Planque & Buffaz 2008) and Ekman transport (anchovy, Irigoien et al. 2008) have been shown to have significant effects on the recruitment or abundance of these species. Therefore, future research is needed to combine the effects of climate variables and food resources in fish biomass, in a trophic approach, to assess future climate change impacts.

8. Concluding remarks

Main climate projections and ecosystem responses

- **Oceanic warming.** Sea surface temperature is expected to increase by 3.5 ^{o}C on average by the end of the century, under the climate change scenario A1B. Expected sea warming is especially severe near the French coast (5.9 ^{o}C).
- **Lower trophic level.** Phytoplankton and zooplankton biomass are expected to increase on average although with a strong spatial variability: (i) on the French shelf, the phytoplankton and zooplankton biomass decrease; (ii) offshore, the

phytoplankton decreases at the centre of the bay and increases elsewhere (south part, and north and west parts) while the zooplankton increases in all the offshore plains; (iii) on the shelf break, both phytoplankton and zooplankton increases.

- **Higher trophic level.** Total fish biomass simulated is expected to increase slightly (4.6%). Anchovy, sardine and hake biomass are expected to increase, whilst the stock of Atlantic mackerel and horse-mackerel is expected to decrease. However, the local decrease of zooplankton biomass in the French shelf, which is the main spawning area in the bay for certain fish species such as European anchovy, could trigger negative consequences for the maintenance of the stock biomass.

Uncertainty of models and projections

Results obtained with ROMS-NPZD model are in agreement with those obtained with POLCOMS-ERSEM for the Bay of Biscay (D3.4 Part 3) in terms of sea warming, although they present slight discrepancies for phytoplankton and zooplankton biomass. The different resolution of the models could explain partially the different results, since the slope is very strong in the Bay of Biscay and the Spanish shelf very narrow.

Additional analyses are necessary to understand *(i)* the role of the physical changes, and especially the stratification, and the role of the shelf break on the ecosystem response; *(ii)* the complex coupled system phytoplankton-zooplankton and especially why zooplankton increases while phytoplankton decreases on the offshore plain; *(iii)* the changes in terms of fish abundance, size and diets (simulated by the HTL model OSMOSE).

Impact to MSFD descriptors

Expected climate change might impact at least five MSFD descriptors (out of 11 defined) of the good environmental status (Table 4):

- **Biological diversity**. Expected changes in phytoplankton and zooplankton biomass are highly variable across the spatial domain, which suggest moderate shifts at species level and slight changes in local diversity.
- **Exploited fish and shellfish**. The expected slight increase in total fish biomass (considering the main 6 exploited fishes) might benefit local fisheries in average, although the stock of Atlantic mackerel and horse-mackerel is expected to slightly decrease. The projections in the higher trophic level are still uncertain.
- **Food webs**. Expected increase in phyto- and zooplankton biomass and their spatial variation triggers positive and negative changes on simulated biomass of the main representative fish species of the bay. This is a well example of how a priori beneficial overall more productive system might alter the food web structure, resulting in winners and also losers.
- **Human-induced eutrophication**. The mean increase of phytoplankton biomass expected by the end of the century could favour eutrophic conditions in those coastal areas already exposed to high nutrient load discharges (Loire, Gironde, *rias* of

Galicia). At present, Galician *rias* experience relevant problems of harmful algal blooms that might be exacerbated with climate change.

- **Hydrographical conditions**. Sea warming is particularly important over the Armorican and Aquitaine shelf, where together with its relatively low depth might intensify the summer stratification.

Access to model results: via MEECE Model Atlas

Table 3. Change of main climate changes and ecosystem response at 2080-2100 relative to 1980-2000 (Scenario A1B) in the Bay of Biscay. Legend: For model uncertainty (based on hindcast validation), Low: the model describes interannual, seasonal and spatial variability appropriately, Medium: the model describes the general observed seasonal and spatial variability, High: the model fails in describing the general pattern (seasonal and spatial). For spatial variability, Low: most of areas with same trends, High: some areas with opposite trends with respect to others. Units: SST (ºC), pH (surface), Phytoplankton (biomass depth integrated) (mg C/m2/d), Zooplankton (biomass depth integrated) (mg C/m2), HTL (total biomass of all fish species considered). Range is expressed in Percentile 25 and Percentile 75. Absolute change for SST. Fractional change for Phytoplankton and Zooplankton biomass and HTL; fractional change = $(A1B_{(2080\text{-}2100)}/PD_{(1980\text{-}2000)})-1$; see Holt et al. (2012); where -1 to 0: decrease, positive values: increase.

	Change range at 2080-2100 relative to 1980-2000				
	SST	pH	Phytoplankton biomass	Zooplankton biomass	HTL OSMOSE
Mean ± Standard Error	3.49±0.09	N/A	0.11±0.03	0.44±0.02	0.05
Test kruskal-Wallis (p-value)	4.32e-08	N/A	0.0013	4.32e-08	
Spatial Range	3.05:3.88	N/A	-0.05:0.23	0.26:0.73	
Spatial variability	Low	N/A	High	High	N/A
Model Uncertainty	Low	N/A	Medium	N/A	High

Table 4. Qualitative descriptors to be used in the environmental status assessment, selected by the European Commission (2010). The second column relates the MEECE outputs for the Bay of Biscay with the MSFD descriptors; thus, it relates the expected impact of climate change to the good environmental status through the MSFD descriptor (indicated by an asterisk).

DESCRIPTOR	MEECE outputs on Climate Change (CC) drivers and Ecosystem response
1: Biological diversity*	- Distribution of biomass of fish species (anchovy, South hake, North hake, sardine, horse-mackerel, Atlantic-mackerel) - Relative proportions of several interacting fish species - Relative proportions of size-based phyto- and zoo-plankton - Sea Temperature, Stratification, Nutrients, defining habitat conditions
2: Non-indigenous species	
3: Exploited fish and shellfish*	- Recruitment for fish species (anchovy) - Biomass of fish species
4: Food webs*	- Abundance of predators such as hake - Abundance trends of fish preys *versus* predators
5: Human-induced eutrophication*	- Nutrients - Phytoplankton biomass
6: Seafloor integrity	
7: Hydrographical conditions*	- Temperature Stratification, upwelling
8: Contaminants	
9: Contaminants in fish and seafood	
10: Litter	
11: Energy and noise	

9. References

Aldanondo, N., Cotano, U., Tiepolo, M., Boyra, G., and Irigoien, X. 2010. Growth and movement patterns of early juvenile European anchovy (*Engraulis encrasicolus* L.) in the Bay of Biscay based on otolith microstructure and chemistry. Fisheries Oceanography, 19: 196-208.

Alheit, J., and Hagen, E. 1997. Long-term climate forcing of European herring and sardine populations. *Fisheries Oceanography*, 6: 130-139.

Allain G, Petitgas P, Lazure P, Grellier P (2007) Biophysical modelling of larval drift, growth and survival for the prediction of anchovy (*Engraulis encrasicolus*) recruitment in the Bay of Biscay (NE Atlantic). *Fish Oceanogr* 16:489–505.

Andonegi, E., Fernandes, J. A., Quincoces, I., Irigoien, X., Uriarte, A., Perez, A., Howell, D., and Stefansson, G. 2011. The potential use of a Gadget model to predict stock responses to climate change in combination with Bayesian networks: the case of Bay of Biscay anchovy. *ICES Journal of Marine Science*, 68: 1257–1269.

Bellier, E., Planque, B. and Petitgas, P. (2007) Historical fluctuations in spawning location of anchovy (*Engraulis encrasicolus*) and sardine (*Sardina pilchardus*) in the Bay of Biscay during 1967–73 and 2000–2004. Fish. Oceanogr. 16:1–15.

Borja, A., Fontan, A., Saenz, J., and Valencia, V. 2008. Climate, oceanography, and recruitment: the case of the Bay of Biscay anchovy (Engraulis encrasicolus). *Fisheries Oceanography*, 17: 477-493.

Chust, G., Caballero, A., Marcos, M., Liria, P., Hernández, C., and Borja, Á. 2010. Regional scenarios of sea level rise and impacts on Basque (Bay of Biscay) coastal habitats, throughout the 21st century. *Estuarine, Coastal and Shelf Science*, 87: 113-124.

Chust G, Borja A, Caballero A, Liria P, Marcos M, Moncho R, Irigoien X, Saenz J, Hidalgo J, Valle M, Valencia V. (2011) Climate Change impacts on the coastal and pelagic environments in the southeastern Bay of Biscay. *Climate Research* 48:307–332.

Fernandes JA, Irigoien X, Goikoetxea N, Lozano JA, Inza I, Pérez A, Bode A (2010) Fish recruitment prediction, using robust supervised classification methods. *Ecol Model* 221: 338–352.

Ferrer, L., A. Fontán, J. Mader, G. Chust, M. González, V. Valencia, Ad. Uriarte, & M. Collins. 2009. Low salinity plumes in the oceanic region of the Basque Country. *Continental Shelf Research* 29:970-984.

Hemery G, D'Amico F, Castege I, Dupont B, D'Elbee J, Lalanne Y, Mouches C (2008) Detecting the impact of oceano-climatic changes on marine ecosystems using a multivariate index: the case of the Bay of Biscay (North Atlantic-European Ocean). *Glob Change Biol* 14:27–38.

Holt, J., Butenschön, M., Wakelin, S. L., Artioli, Y., and Allen, J. I. (2012) Oceanic controls on the primary production of the northwest European continental shelf: model experiments under recent past conditions and a potential future scenario, *Biogeosciences*, 9, 97-117,

Holt, J., Wakelin, S., Lowe, J. & Tinker, J. (2010) The potential impacts of climate change on the hydrography of the northwest European continental shelf. *Progress in Oceanography*, 86, 361-379.

Irigoien X, Cotano U, Boyra G, Santos M and others (2008) From egg to juvenile in the Bay of Biscay: spatial patterns of anchovy (Engraulis encrasicolus) recruitment in a nonupwelling region. *Fish Oceanogr* 17:446–462.

Kalnay et al. 1996. “The NCEP/NCAR 40-year reanalysis project”. Bull. Amer. Meteor. Soc., 77, 437-470.

Lazure P., Dumas F. & Vrignaud C., 2008. “Circulation on the Armorican shelf (Bay of Biscay) in autumn”. J. Mar. Sys., doi:10.1016/j.jmarsys.2007.09.011.

Motos, L. (1996) Reproductive biology and fecundity of the Bay of Biscay anchovy population (Engraulis encrasicolus L.). Sci. Mar. 60(Suppl. 2):195–207.

Planque B, Buffaz L (2008) Quantile regression models for fish recruitment–environment relationships: four case studies. *Mar Ecol Prog Ser* 357:213–223.

Richardson, A. J. 2008. In hot water: zooplankton and climate change. – ICES Journal of Marine Science, 65: 279–295.

Shchepetkin, A. F. and J. C. McWilliams, 2005: The regional ocean modeling system (ROMS): A split-explicit, free-surface, topography-following-coordinate oceanic model. *Ocean Modeling* **9**/4, pp. 347-404, doi:10.1016/j.ocemod.2004.08.002

Smith, W. H. F. & Sandwell D. T. (1997). “Global seafloor topography from satellite altimetry and ship depth soundings”. *Science* 277, 1957-1962, 26 Sept 1997.

Taylor, K. E., 2001. “Summarizing multiple aspects of model performance in a single diagram”. Journal of Geophysical Research, 106: 7183-7192.